The role of dark matter halos in the motion of stars in galaxies

Author: Jordi de la Barrera Bardalet
Facultat de Física, Universitat de Barcelona, Diagonal 645, 08028 Barcelona, Spain

Advisor: Alberto Manrique Oliva

Abstract: In this paper, we study the effects produced by a dark matter halo on the regular or chaotic nature of the orbits of a star moving near the galactic plane. The potential consists of three components: a spherical core, a disk and an ellipsoidal dark matter halo. We run simulations with three different halo shapes at three different energies. Using Poincaré sections we visually analyze the transition from regular to chaotic orbits and confirm that the shape of the dark halo is a key element: the spherical halo keeps the orbits stable, the prolate halo induces more chaotic orbits globally while the triaxial ellipsoid only does so at the core.

I. INTRODUCTION

Dark matter halos are in the present moment of extreme relevance in galactic dynamic studies as more complex systems are arising and new questions need to be answered. Although they cannot be seen directly and we don't know their exact shape, we cannot omit the interaction a dark halo has with the stars in the galaxy, as it is the primary gravity source that rules galactic dynamics, thus, star motion.

There are plenty of studies that try to fit a halo model that is compatible with the real observations (Law et al. (2010)[1]). In the present paper however, we take the opposite approach: choosing three realistic halos with different shapes we analyze how the motion of the stars is affected and what are the differences between each halo effects. This paper follows the studies of Hénon & Heyles (1964)[3] on the existance of a third isolating integral that led to the orbits of the stars transition from regular to chaotic. They analyzed this transition using an arbitrary potential which did not represent any galactic potential. Following their methodology, we study the transition with a real galactic potential with three components taken from Law et al. (2010)[1], one of them being a dark matter halo.

Firstly, we take three cases of halo shapes: a triaxial ellipsoid, a shpere and lastly a prolate ellipsoid (rugby ball shape). We then integrate a set of initial conditions at three different energies and compute the Poincaré sections in the $(y, \dot{y})$ plane, which are 2D projections of the evolution of the particle in the phase space. This study provides a qualitative understanding of the halo effects in the motion of a star near the disk.

This paper is structured as follows. Section II starts by describing the galactic potential model and gives a detailed description of each of the parameters, equations of motion and constraints of the system. It also includes a brief explanation on the computational methodology and how Poincaré sections are constructed. In Section III we show the results analyzing the Poincaré sections for each case and energy. Finally in Section IV we present the results with the conclusions.

II. EQUATIONS

A. The galactic model

The galactic potential used in this paper is taken from Law et al. (2010) [1]. It is composed by three components: a Hernquist spheroid as the core, a disk, and a triaxial dark matter halo modeling the Milky Way potential with its characteristic parameters. The disk component is described by the potential used in Miyamoto & Nagai (1975) [2]. Thus,

$$\Phi = \Phi_{sphere} + \Phi_{disk} + \Phi_{halo}, \tag{1}$$

Where each component is given by the following expressions:

$$\Phi_{sphere} = -\frac{GM_{sphere}}{\sqrt{x^2+y^2+z^2}+c_s}, \tag{2}$$

$$\Phi_{disk} = -\frac{GM_{disk}}{\sqrt{x^2+y^2+\left(a_d+\sqrt{z^2+b_d^2}\right)^2}}, \tag{3}$$

$$\Phi_{halo} = v_{halo}^2 ln\left(r_{halo}^2 + C_1x^2 + C_2y^2 + C_3xy + \left(\tfrac{z}{q_z}\right)^2\right), \tag{4}$$

While the constants of the dark halo are given by:

$$C_1 = \left(\frac{\cos^2\phi}{q_1^2} + \frac{\sin^2\phi}{q_2^2}\right), \tag{5}$$

$$C_2 = \left(\frac{\cos^2\phi}{q_2^2} + \frac{\sin^2\phi}{q_1^2}\right), \tag{6}$$

$$C_3 = 2\sin\phi\cos\phi\left(\frac{1}{q_1^2} - \frac{1}{q_2^2}\right), \tag{7}$$

The parameters a_d and b_d caracterize the central concentration and the thickness of the disk, respectively, and c_s refers to the radius of the spherical core.

The dark matter halo represented in this form describes an ellipsoid with major/intermediate/minor semi-axes a/b/c rotated by an angle ϕ about the Galactic Z-axis. Both q_1 and q_2 denote the axial flattening of the disk axis while q_z does so with the axis perpendicular to the Galactic disk. We take the origin $\phi = 0^o$ in the case where q_1 and q_2 are coincident with the Galactic X/Y axes and it increases in the direction of the Galactic longitude. Finally, v_{halo} is the normalization parameter of the total mass of the dark halo and r_{halo} is a scale length.

This study is developed in units of kpc for distances, solar masses and Myrs for time. Thus, the resulting units of the energy are $[E] = kpc^2 Myr^{-2} M_\odot^{-1}$, which in fact corresponds to an energy per mass unit, as it can be easily seen in Eq. (4) which has velocity squared dimensions per unit of mass. From now on, we will drop the $M_\odot^{-1}$ when writing energy units.

B. Equations of motion

Taking the three components of the potential we can write the Hamiltonan of the system:

$$H = \frac{1}{2}\left(p_x^2 + p_y^2 + p_z^2\right) + \Phi\left(x, y, z\right), \tag{8}$$

As we work with Cartesian coordinates the equations of motion are given by:

$$\ddot{x} = -\frac{\partial \Phi}{\partial x}, \ddot{y} = -\frac{\partial \Phi}{\partial y}, \ddot{z} = -\frac{\partial \Phi}{\partial z}, \tag{9}$$

The phase space $(x, y, z, \dot{x}, \dot{y}, \dot{z})$ has six dimensions and one isolating integral that is known, which is the total energy of the star divided by its mass, that is constant through all the trajectory of the star:

$$I_1 = \frac{1}{2}\left(\dot{x}^2 + \dot{y}^2 + \dot{z}^2\right) + \Phi\left(x, y, z\right), \tag{10}$$

Because of the existence of this isolating integral it is only necessary to know five of the coordinates in the phase sphace such as $x, y, z, \dot{y}, \dot{z}$; then, the sixth component, $\dot{x}$, can be obtained from Eq. (10) using $I_1 = E$, the total energy of the star.
Considering that $\dot{x}$ must be non-negative this defines a volume in the phase space where the star can evolve. If no other isolating integrals exist, the star will move and fill all this volume and the trajectory will be cahotic or also named ergodic. However, the trajectory will lie on a surface in case of the existance of a second isolating integral, which is what this paper aims to show.
As it will be seen futher ahead, when plotting the Poincaré sections this two behaviours of the trajectories will correspond to the following: ergodic trajectories filling an area and regular orbits laying in a curve.

C. Computational methodology

To compute the calculations of the trajectory of each star, the equations of motion have been integrated using an Adaptative Runge Kutta method in Fortran [4] which varies the integration step lenght conveniently, optimizing to reduce both error and CPU time. A precision of 10^{-6} has been acheived with an integration time of 10^5 Myr with a number of 10^7 steps.
In order to make sure of the reliability of the integration method, the study by Hénnon & Heiles (1964) [3] has been previously reproduced successfully.

In the present study, the integration of the equation of motion Eq. (9) has been used to compute the Poincaré sections in the $y, \dot{y}$ plane. These sections have been generated by the succesion of points of the trajectory $P_1, P_2, ...$ that intersect with the $x = 0$ plane, in the upward direction, which implies that:

$$x = 0, \dot{x} > 0, \tag{11}$$

Only points with $|z| < 0.02kpc$ are represented, this is, points that move near the galactic equatorial plane. As previously stated, these points will draw a closed curve given the existance of a second isolating integral of motion. In that case we will call these trajectories regular.

On the other hand, if a second isolating integral of motion doesn't exist the points will be distributed filling an area instead, and the orbits will be called ergodic (see Fig.1(g) for a clear view of the difference between ergodic and regular orbits in a Poincaré section).

In order to integrate the equations of motion Eq.(9), we first define the first four initial components, which are common for all the starting points. Thus, we set $x = z = \dot{y} = \dot{z} = 0$. Components z and $\dot{z}$ are set to zero with the goal of studying stars that move in the equatorial plane. Then, an array of unique y components is created and finally the sixth component, $\dot{x}$, is found by using the energy conservation isolating integral of Eq.(10). We then integrate the equations of motion with the initial condition of each trajectory, which allows us to compute the Poincaré sections.

III. RESULTS

A. Effects of the dark halo's shape

The aim of this section is to study the effects in the nature of the orbits produced by three realistic halo shapes. Specifically, it is of our interest to distinguish between regular and ergodic orbits as a function of the energy. For each case, we integrated three sets of initial conditions at three different energies: 0.15, 0.22 and 0.28 kpc^2Myr^{-2} and computed the corresponding Poincaré sections in the plane $(y, \dot{y})$.

Parameter	Value
$M_{sphere}(M_\odot)$	1.0×10^{11}
$M_{disk}(M_\odot)$	3.4×10^{10}
$a_d(kpc)$	6.5
$b_d(kpc)$	0.26
$c_s(kpc)$	0.7
$r_{halo}(kpc)$	12
$v_{halo}(km/s)$	220
$\phi(^o)$	90

Parameter	Case 1	Case 2 (Spherical)	Case 3 (Prolate)
q_1	0.83	1.0	3.0
q_2	1.0	1.0	1.0
q_z	0.67	1.0	0.5
T	0.55	1	0.91

TABLE I: Parameters used for calculations. The oblate case has been ommited here because prolate cases were found to be more relevant for this particular study. T is the triaxiallity parameter defined in Eq. (12).

In Table I the parameters that we used for each case have been listed. The parameters from the table on top are common for all cases and were taken from Law et al. (2010) [1] while the shape parameters of the three halos displayed in this study are set on the lower table in Table I.

Once all parameters are defined, we should have a method to classify each halo type by its shape. The best method is the triaxiallity parameter, defined by:

$$T = \frac{a^2 - b^2}{a^2 - c^2}, \tag{12}$$

where T $\rightarrow$ 0 means it is an oblate ellipsoid with $a \simeq b > c$ (Earth-type ellipsoid) and T $\rightarrow$ 1 means it is prolate with $a > b \simeq c$ (like the shape of a rugby ball). A spherical shaped halo has also been studied and it corresponds to $a = b = c$ with T=1. To find the triaxiality value of a given ellipsoid we set a/b/c equal to the highest/intermediate/lowest of the values from q_1, q_2 and q_z.

That way, this paper focuses on three halo shapes with T=0.55, 1 and 0.91 corresponding to a triaxial ellipsoid, a sphere and a prolate ellipsoid, respectively.

In Figure 1 the Poincaré sections are represented for the three shapes and energies. Each of the orbits was obtained from a different initial condition for a given energy, integrated and followed in the phase space.

Starting with Figure 1(a), which shows the Poincaré section for the case T=0.55 at E=0.15 $(kpc/Myr)^2$, at a first glance we observe the symmetry of the galactic potential in y. It is easily seen that the orbits are all regular, following closed curves and filling all the allowed area. It is also noticeable the presence of three invariant points in the middle of the three loops: one at y=0 which is hard to see here and the other two at the sides. These points correspond to stable and periodic orbits.

As discussed in Section II, the presence of closed curves in the Poincaré section indicates the existance of a second isolating integral.

In Figure 1(b) the central loop has increased in size but it seems that all the orbits are still regular including the ones with missing points. If we were to increase the integration time we could probably verify that the orbits end up closing themselves. However, Figure 1(c) for E=0.28 $(kpc/Myr)^2$ shows a totally different behaviour at the core. What before were closed orbits that filled the whole area with curves, now the points are scattered and filling most of the area without any kind of order. Besides that, we still observe the presence of regular orbits at the core in the form of the six small islands, 3 in dark blue and another three in orange, and probably more islands that can be intuited inside the four white spaces close to the center. What is surprising is that all the islands of the same color belong to the same trajectory: the star jumps from one island to the other as it turns around the galaxy.

Another effect of the rise in energy is that the range of positions y also rises with the star moving further away from the center at higher energies.

When compared, the only difference between the section of Figure 1(b), from the spherical halo, and Figure 1(a) is the absence of the central loop. Besides that, like in the previous case all the orbits seem to be regular and there are equally two stable points. Going at higher energies nothing much changes. As before, the range in y increases, but in this case all orbits keep being regular, even for the highest energy. Out of the three studied cases, the spherical one has turned out to be the one showing the least effects in the orbits of the stars.

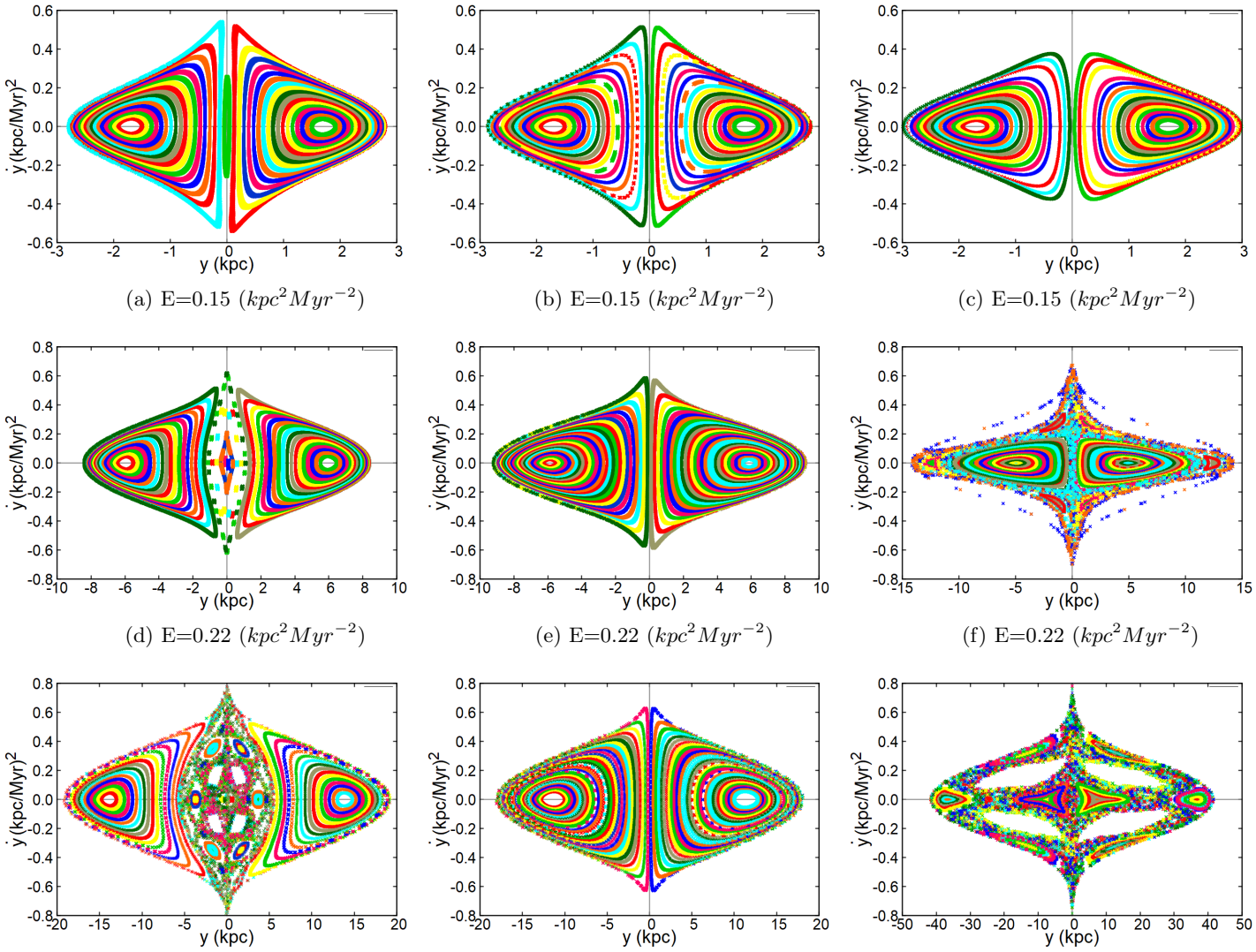

(a) E=0.15 ($kpc^2 Myr^{-2}$) (b) E=0.15 ($kpc^2 Myr^{-2}$) (c) E=0.15 ($kpc^2 Myr^{-2}$)

(d) E=0.22 ($kpc^2 Myr^{-2}$) (e) E=0.22 ($kpc^2 Myr^{-2}$) (f) E=0.22 ($kpc^2 Myr^{-2}$)

(g) E=0.28 ($kpc^2 Myr^{-2}$) (h) E=0.28 ($kpc^2 Myr^{-2}$) (i) E=0.28 ($kpc^2 Myr^{-2}$)

FIG. 1: Poincaré sections at different energies for three dark halo shapes using the parameters described in Table I. From left to right: triaxial halo (T=0.55), spherical (T=1) and prolate (T=0.91).

In contrast, the highly prolate halo of case 3, with T=0.91, has a huge impact on the motion of stars. This halo has $q_1 = 3$, which is much bigger than the other two axis.

Due to the rotation of $\phi = 90^o$, q_1 is aligned to the Galactic Y-axis, massively elongating the orbits along that axis as it can be seen in Figures 1(f) and 1(i).

At the lowest energy there are not any remarkable differences from the previous cases. However, stepping up to E=0.22 $(kpc/Myr)^2$ we observe that the regular orbits have now compressed vertically and streatched horizontally, reaching points 5 kpc further from the center than the previous cases. Already at this energy, the axis y=0 together with other areas have become chaotic regions which was an unseen behaviour compared with the previous two at this energy.

Groups of regular islands, also known as chain islands, are also present. The white space between the boundary of the Poincaré section in color blue and the chaotic area is probably a region of regular orbits. Had we chosen an initial condition inside this area, not with $\dot{y} = 0$ as we have in this case, we could have this hypothesis verified, although it can also be done by looking at Figure 1(i) and confirming the presence of regular orbits in that region.

Finally, in Figure 1(i) the regular region at the center shrinks considerably and the white area seems to move closer to the center. Moreover, we can observe another unseen behaviour. Up to this point, we have only seen reductions of the regular regions as the energy is increased. Surprisingly, looking at the side edges we observe two little regular regions from Figure 1(f) that have increased in size in Figure 1(i), which makes us think that if we were to increase the energy even more we could have more regular regions.

IV. CONCLUSIONS

This paper's goal was to study whether the shape of the dark halo had an effect on the star motion and how it affected the nature of it. The results in Section III allow us to conclude that:

- First, the shape of the dark matter halo is a key element that drives the dynamics of the stars near the equatorial plane, which reinforces the importance of following with further studies on the topic.
- Secondly, we observed that energy plays an imporant role on the transition from regular to chaotic orbits. Over a certain energy there are regions where the second isolating integral ceseases to exist and the orbits in that region become chaotic.
- The three studied shapes have given completely different orbits. The spherical halo (T=1) seems to make orbits stable even at high energies, the prolate ellipsoid (T=0.91) induces chaotic orbits globally and it's the one affecting the most and finally, the triaxial halo (T=0.55) produces transformations from regular to chaotic orbits only near the center.

The present paper has taken a qualitative approach to the problem. One remaining question is, at what energy do the orbits start to become chaotic. A quantitative study could be done following Hénon & Heyles methodology of the fraction of area developed in [3] and use it to find the most altering shapes of the halo.

Acknowledgments

I would like to finish giving appreciation to my tutor Prof. Alberto Manrique. His willigness to help and full disponibility during the semester have been of great help for me. To my family and close friends for being there everytime I needed them.

[1] Law, D.R., Majewski, S. R. 2010, ApJ, 714, 229.
[2] Miyamoto,M., & Nagai, R. 1975, PASJ, 27, 533.
[3] Hénon, M., Heiles, C. 1964, AJ, 69, 73.
[4] W. H. Press, W. T. Vetterling, S. A. Teukolsky, B. P. Flannery, *Numerical Recipies in Fortran*, (Cambridge University Press, Cambridge 1992).